

# ${}^3_{\Lambda}\text{H}$ and ${}^4_{\Lambda}\text{H}$ Lifetime, Yield, Directed Flow Measurements in Au+Au Collisions at $\sqrt{s_{NN}} = 3$ GeV With the STAR Detector

Chenlu Hu<sup>1,\*</sup> for STAR collaboration

<sup>1</sup>Quark Matter Research Center, Institute of Modern Physics, Chinese Academy of Sciences

**Abstract.** In this proceedings, the lifetime and yields of  ${}^3_{\Lambda}\text{H}$  and  ${}^4_{\Lambda}\text{H}$  in Au+Au collisions at  $\sqrt{s_{NN}} = 3$  GeV are presented. The measured yields are compared to measurements at other energies and theoretical models, and the physics implications are discussed. We also report the first observation of the  ${}^3_{\Lambda}\text{H}$  and  ${}^4_{\Lambda}\text{H}$  directed flow in 5 - 40% centrality. The directed flow of  ${}^3_{\Lambda}\text{H}$  and  ${}^4_{\Lambda}\text{H}$  are compared with those of the copiously produced particles such as p,  $\Lambda$ , d, t,  ${}^3\text{He}$ , and  ${}^4\text{He}$ . These results shed light on light hyper-nuclei production in heavy-ion collisions in the high baryon density region.

## 1 Introduction

As is known to all, the normal nucleus is made up of protons and neutrons. When a nucleon is replaced by a  $\Lambda$  hyperon ( $S = -1$ . Here  $S$  denotes the quantum number of strangeness), the nucleus is transformed into a hyper-nucleus which allows us to study the hyperon-nucleon (Y-N) interaction. It is well known that 2-body and 3-body Y-N interactions, especially at high baryon density, are essential for understanding the inner structure of compact stars [1-2]. Measurements of the lifetime, binding energy, decay branching ratios of hyper-nuclei can give us important information on Y-N interaction.

Anisotropic flow has been commonly used for studying the properties of matter created in high energy nuclear collisions, due to its genuine sensitivity on early stage collision dynamics [3]. The first order coefficient of the Fourier-expansion of azimuthal distribution, known as directed flow ( $v_1$ ), has been analyzed for all particles ranging from the lightest pion-mesons to light nuclei in such collisions [4-5].

In this proceedings, the lifetime, yields and directed flow of  ${}^3_{\Lambda}\text{H}$  and  ${}^4_{\Lambda}\text{H}$  in Au+Au collisions at  $\sqrt{s_{NN}} = 3$  GeV will be discussed. The data was collected by the STAR experiment at RHIC with the fixed-target (FXT) setup. The gold beam of 3.85 GeV/u is collided on a thin gold target with 1% interaction probability, located at 200 cm along the beam direction from the center of the STAR Time-Projection Chamber (TPC). A total of 260M good minimum bias (MB) events were selected for this analysis.

## 2 Data Analysis, Results and Discussion

At the  $\sqrt{s_{NN}} = 3$  GeV collisions, the first order event plane is determined by the Event Plane Detector (EPD) [6], which is designed to measure the pattern of forward-going charged

---

\*e-mail: [huchenlu@impcas.ac.cn](mailto:huchenlu@impcas.ac.cn)

particles emitted in heavy-ion collisions and covers a pseudorapidity range of  $2.14 < |\eta| < 5.09$ . The directed flow ( $v_1$ ) discussed below is determined by the first order event plane.

## 2.1 Particle Reconstruction

The hyper-nuclei  ${}^3_{\Lambda}\text{H}$  and  ${}^4_{\Lambda}\text{H}$  are reconstructed with following decay channels:  ${}^3_{\Lambda}\text{H} \rightarrow {}^3\text{He} + \pi^-$ ,  ${}^3_{\Lambda}\text{H} \rightarrow \text{d} + \text{p} + \pi^-$ ,  ${}^4_{\Lambda}\text{H} \rightarrow {}^4\text{He} + \pi^-$ . To assure the quality of each track, a minimum of 15 hits out of 45 hits in the TPC is required. The secondary decay topology is reconstructed by the KFPparticle program which is based on a Kalman filter method [7]. In the program, the error-matrices are used to enhance the reconstruction significance. A set of cuts on topological variables are applied to the hyper-nuclei candidates to optimize the significance.

## 2.2 ${}^3_{\Lambda}\text{H}$ and ${}^4_{\Lambda}\text{H}$ Lifetime Measurements

The reconstructed  ${}^3_{\Lambda}\text{H}$  and  ${}^4_{\Lambda}\text{H}$  candidates are divided into different  $L/\beta\gamma$  intervals, where  $L$  is the decay length,  $\beta$  and  $\gamma$  are particle velocity and Lorentz factor, respectively. The raw signal counts  $N^{raw}$  for each  $L/\beta\gamma$  interval are obtained from corresponding background-subtracted invariant mass spectrum using a bin counting method. The signal counts are corrected with the detector acceptance and reconstruction efficiency ( $\epsilon_{TPC} \times \epsilon_{PID}$ ). The corrected hyper-nuclei counts as a function of  $L/\beta\gamma$  is fitted to an exponential function ( $N = N_0 e^{-L/\beta\gamma\tau}$ ) to obtain the mean lifetime  $\tau$ .

The lifetimes  $232 \pm 29(\text{stat.}) \pm 37(\text{syst.})$  for  ${}^3_{\Lambda}\text{H}$  (2-body decay channel) and  $218 \pm 8(\text{stat.}) \pm 12(\text{syst.})$  for  ${}^4_{\Lambda}\text{H}$  are obtained from the  $\sqrt{s_{NN}} = 3$  GeV data. As shown in Fig. 1, the  ${}^4_{\Lambda}\text{H}$  measurement is the most precise measurement to date, and within uncertainties, the measured  ${}^3_{\Lambda}\text{H}$  and  ${}^4_{\Lambda}\text{H}$  lifetimes are consistent with previous measurements from ALICE [8, 9], STAR [10], HypHI [11].

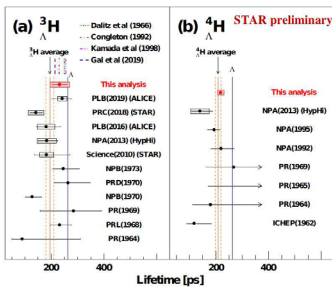


**Figure 1.** Measured lifetimes of  ${}^3_{\Lambda}\text{H}$  (a) and  ${}^4_{\Lambda}\text{H}$  (b) are shown comparing to previous measurements and theoretical calculations as well as the free  $\Lambda$  lifetime. The experimental average lifetimes and the corresponding uncertainty of  ${}^3_{\Lambda}\text{H}$  and  ${}^4_{\Lambda}\text{H}$  are also shown as orange bands.

## 2.3 ${}^3_{\Lambda}\text{H}$ and ${}^4_{\Lambda}\text{H}$ Yield Measurements

The hyper-nuclei  ${}^3_{\Lambda}\text{H}$  and  ${}^4_{\Lambda}\text{H}$  yields from their 2-body decay channels are extracted as a function of  $p_T$  and  $y$  in two centrality selections: 0–10% and 10–50%. The efficiency-corrected  $p_T$  spectra in each rapidity slice are extrapolated down to  $p_T=0$  to obtain  $p_T$  integrated value of yields ( $dN/dy$ ). Different functions (e.g blast-wave function) are used to estimate the systematic uncertainties in the unmeasured  $p_T$  regions. We have assumed branching ratios of 25% and 50% for the 2-body decay of  ${}^3_{\Lambda}\text{H}$  and  ${}^4_{\Lambda}\text{H}$ , respectively.

The  ${}^3_{\Lambda}\text{H}$  and  ${}^4_{\Lambda}\text{H}$  yields at  $|y| < 0.5$  as a function of beam energy in central heavy-ion collisions are extracted and are compared to theoretical models as shown in Fig. 2. For  ${}^3_{\Lambda}\text{H}$ , the measured yield is consistent with the thermal model from GSI/Heidelberg [12]. The thermal model adopting the canonical ensemble can approximately describe the  ${}^3_{\Lambda}\text{H}$  yield

both at 3 GeV and 2.76 TeV. Canonical ensemble thermal statistics is required to account for the large  $\phi/K^-$  and  $\phi/\Xi^-$  ratios measured at the same energy as well. We also observe that the coalescence model (DCM) [13] is consistent with the  ${}^3_{\Lambda}\text{H}$  yield while underestimating the  ${}^4_{\Lambda}\text{H}$ . On the other hand, the hybrid UrQMD overestimates both  ${}^3_{\Lambda}\text{H}$  and  ${}^4_{\Lambda}\text{H}$  yields by an order of magnitude.

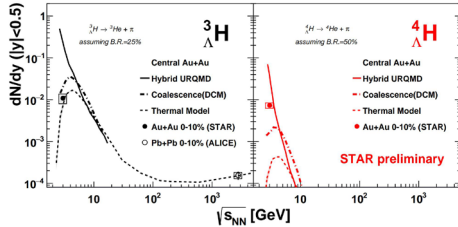


**Figure 2.**  ${}^3_{\Lambda}\text{H}$  (a) and  ${}^4_{\Lambda}\text{H}$  (b) yields at  $|y| < 0.5$  as a function of beam energy in central heavy ion collisions. The symbols represent measurements while the lines represent different theoretical calculations. The data points assume a branching ratio of 25(50)% for  ${}^3_{\Lambda}\text{H}({}^4_{\Lambda}\text{H}) \rightarrow {}^3\text{He}({}^4\text{He}) + \pi^-$ .

## 2.4 ${}^3_{\Lambda}\text{H}$ and ${}^4_{\Lambda}\text{H}$ Directed Flow Measurements

Directed flow of  $\Lambda$  hyperons,  ${}^3_{\Lambda}\text{H}$ , and  ${}^4_{\Lambda}\text{H}$  are extracted with event plane method. Figure 3 shows the  $v_1$  for hyper-nuclei and  $\Lambda$  hyperons versus rapidity from the  $\sqrt{s_{NN}} = 3$  GeV Au + Au collisions. The yellow-red line is the result of linear fit to the data and is plotted in full rapidity region  $|y| \leq 0.9$ . For comparison, the  $v_1$  distributions for p, d, t,  ${}^3\text{He}$  and  ${}^4\text{He}$ , from the events with same centrality, are shown as open symbols in the figure. Here the results of the linear fits to the light-nuclei are plotted as dashed-lines only in the positive rapidity region. As one can see, the  $v_1$  of  $\Lambda$  hyperons is consistent with that of protons, and the slopes of hyper-nuclei  $v_1$  are also similar to that of the corresponding light-nuclei with the same mass number within statistical uncertainties.

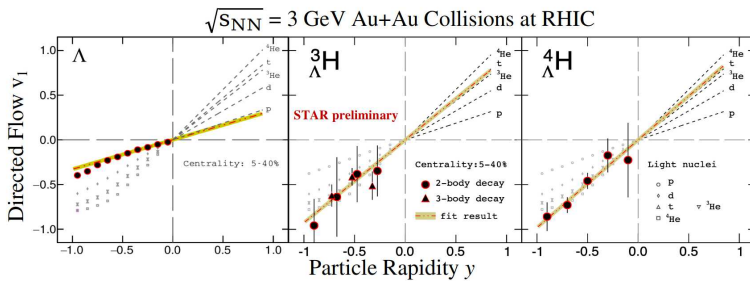


**Figure 3.** Hyper-nuclei  $v_1$  as a function of rapidity from the  $\sqrt{s_{NN}} = 3$  GeV 5 – 40% mid-central Au + Au collisions at RHIC-STAR. In case of  ${}^3_{\Lambda}\text{H}$ , both 2-body (dots) and 3-body (triangles) decays are used. Results from fitting with a first-order polynomial function are shown as the yellow-red lines. The rapidity dependence of  $v_1$  for p, d, t,  ${}^3\text{He}$  and  ${}^4\text{He}$  are also shown as open-circles, up-triangles, down-triangles and squares, respectively. The corresponding results of the linear fits are shown as dashed lines in the positive rapidity region.

Extracted mid-rapidity  $v_1$  slopes,  $dv_1/dy|_{y=0}$ , for  $\Lambda$  hyperons,  ${}^3_{\Lambda}\text{H}$ , and  ${}^4_{\Lambda}\text{H}$ , are summarized in Fig. 4 as red filled-squares, as a function of particle mass. For comparison, the slopes of light-nuclei p, d, t,  ${}^3\text{He}$ , and  ${}^4\text{He}$  from the events with same centrality class (5-40%) in  $\sqrt{s_{NN}} = 3$  GeV Au+Au collisions are shown as open circles. The result of a linear fit to the light-nuclei is shown as the yellow-red line in the figure. Overall, hyper-nuclei  $v_1$  slopes are consistent with that of light-nuclei which has similar mass albeit the large uncertainties in the results. The mass dependence of the  $v_1$  slope implies that the coalescence is the dominant mechanism for hyper-nuclei production in heavy-ion collisions.

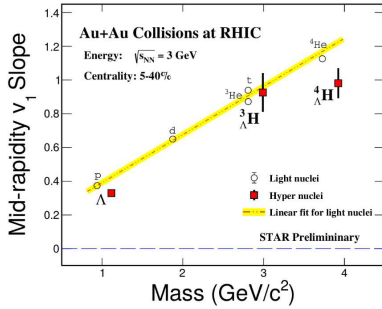


**Figure 4.** Mass dependence of the mid-rapidity  $v_1$  slope  $dv_1/dy|_{y=0}$  for  $\Lambda$ ,  ${}^3_{\Lambda}\text{H}$  and  ${}^4_{\Lambda}\text{H}$ , from the  $\sqrt{s_{NN}} = 3$  GeV mid-central 5-40% Au+Au collisions. Combined results of 2-body and 3-body decays are used for  ${}^3_{\Lambda}\text{H}$  while the  ${}^4_{\Lambda}\text{H}$  is only reconstructed from the 2-body decay. The slopes of light-nuclei p, d, t,  ${}^3\text{He}$  and  ${}^4\text{He}$  from the same collisions are shown as open circles. The yellow-red line is the result of a linear fit to the measured light nuclei  $v_1$  slopes.

### 3 Summary

In summary, we reconstruct the light hyper-nuclei  ${}^3_{\Lambda}\text{H}$  and  ${}^4_{\Lambda}\text{H}$  from  $\sqrt{s_{NN}} = 3$  GeV Au+Au collisions at RHIC-STAR. Lifetimes of  ${}^3_{\Lambda}\text{H}$  and  ${}^4_{\Lambda}\text{H}$  from their 2-body decay channel are measured to be  $232 \pm 29(\text{stat.}) \pm 37(\text{syst.})$  and  $218 \pm 8(\text{stat.}) \pm 12(\text{syst.})$  respectively. The  ${}^3_{\Lambda}\text{H}$  and  ${}^4_{\Lambda}\text{H}$  lifetimes are consistent with previous measurements and theoretical calculations. Meanwhile, the hyper-nuclei  ${}^3_{\Lambda}\text{H}$  and  ${}^4_{\Lambda}\text{H}$  yields at  $|y| < 0.5$  as a function of beam energy in central heavy-ion collisions are reported and compared to theoretical models. We also reported the first observation of  ${}^3_{\Lambda}\text{H}$  and  ${}^4_{\Lambda}\text{H}$  directed flow  $v_1$  from mid-central (5-40%) collisions. The rapidity dependence of their  $v_1$  are compared with that of  $\Lambda$  hyperon and light nuclei p, d, t,  ${}^3\text{He}$  and  ${}^4\text{He}$  from the collisions with the same centrality class. It is found that, within statistical uncertainties, the mid-rapidity  $v_1$  slope of  ${}^3_{\Lambda}\text{H}$  and  ${}^4_{\Lambda}\text{H}$  are similar to those of light nuclei with the similar mass, such as t,  ${}^3\text{He}$ , and  ${}^4\text{He}$ . In other words, they seem to follow the baryon mass scaling. These observations imply that coalescence of nucleons and  $\Lambda$  hyperons is the dominant mechanism for the light hyper-nuclei production in such collisions.

### 4 Acknowledgments

We thank Drs. Y. Nara and J. Steinheimer for interesting discussions and the use of simulations code of JAM and UrQMD.

### References

- [1] D. Gerstung, N. Kaiser, and W. Weise, Eur. Phys. J. **A56**, 175 (2020)
- [2] D. Lonardonni et al., Phys. Rev. Lett. **114**, 092301 (2015)
- [3] C.M. Hung and E. Shuryak, Phys. Rev. Lett. **75**, 4003 (1995)
- [4] L. Adamczyk et al. (STAR Collaboration), Phys. Rev. Lett. **112**, 162301 (2014)
- [5] M.S. Abdallah et al. (STAR Collaboration), Phys. Rev. **C103**, 034908 (2021)
- [6] J. Adams et al. (STAR Collaboration), NIM **A968**, 163970 (2020)
- [7] I. Kisel et al. (CBM Collaboration), J. Phys. Conf. Ser. **1070**, 012105 (2018)
- [8] S. Acharya et al. (ALICE), Phys. Lett. B **797**, 134905 (2019), 1907.06906.
- [9] J. Adam et al. (ALICE), Phys. Lett. B **754**, 360 (2016), 1506.08453.
- [10] L. Adamczyk et al. (STAR), Phys. Lett. C **97**, 054909 (2018), 1710.00436.
- [11] C. Rappold et al., Nucl. Phys. A **913**, 170 (2013), 1305.4871.
- [12] A. Andronic, Phys. Lett. B **679**, 203 (2011), 1010.2995.
- [13] J. Steinheimer, K. Gudima, A. Botvina, I. Mishustin, M. Bleicher, and H. Stoecker, Phys. Lett. B **714**, 85 (2012), 1203.2547.